

# Ammonium transformation in a nitrogen-rich tidal freshwater marsh

Britta Gribsholt · Eric Struyf · Anton Tramper · Maria G. I. Andersson ·  
Natacha Brion · Loreto De Brabandere · Stefan Van Damme · Patrick Meire ·  
Jack J. Middelburg · Frank Dehaers · Henricus T. S. Boschker

Received: 21 July 2005 / Accepted: 27 March 2006  
© Springer Science+Business Media B.V. 2006

**Abstract** The fate and transport of watershed-derived ammonium in a tidal freshwater marsh fringing the nutrient rich Scheldt River, Belgium, was quantified in a whole ecosystem  $^{15}\text{N}$  labeling experiment. In late summer (September) we added  $^{15}\text{N-NH}_4^+$  to the flood water entering a 3477 m<sup>2</sup> tidal freshwater marsh area, and traced the ammonium processing and retention in four subsequent tide cycles. In this paper we present the results for the water-phase components of the marsh system and compare them to a similar experiment conducted in spring/early summer (May). Changes in concentration and isotopic enrichment of  $\text{NO}_3^- + \text{NO}_2^-$ ,  $\text{N}_2\text{O}$ ,  $\text{N}_2$ ,  $\text{NH}_4^+$  and suspended particulate nitrogen (SPN) were measured in concert with a mass balance study. All

analyzed N-pools were labeled, and 49% of the added  $^{15}\text{NH}_4^+$  was retained or transformed. The most important pool for  $^{15}\text{N}$  was nitrate, accounting for 17% of  $^{15}\text{N}$ -transformation.  $\text{N}_2$ ,  $\text{N}_2\text{O}$  and SPN accounted for 2.4, 0.02 and 1.4%, respectively. The temporal and spatial patterns of  $^{15}\text{N}$  transformation in the water phase component of the system were remarkably similar to those observed in May, indicating good reproducibility of the whole ecosystem labeling approach, but the absolute ammonium transformation rate was 3 times higher in May. While the marsh surface area was crucial for nitrification in May this was less pronounced in September. Denitrification, on the other hand, appeared more important in September compared to May.

B. Gribsholt (✉) · A. Tramper ·  
M. G. I. Andersson · J. J. Middelburg ·  
H. T. S. Boschker  
Center for Estuarine and Marine Ecology,  
Netherlands Institute of Ecology (NIOO-KNAW),  
P.O. Box 140, 4400 AC Yerseke, The Netherlands  
e-mail: B.Gribsholt@nioo.knaw.nl

E. Struyf · S. Van Damme · P. Meire  
Department of Biology, Ecosystem Management  
Research Group, Universiteit Antwerpen,  
Universiteitsplein 1, B-2160 Wilrijk, Belgium

N. Brion · L. De Brabandere · F. Dehaers  
Department of Analytical and Environmental  
Chemistry, Vrije Universiteit Brussel, Pleinlaan 2,  
B-1050 Brussel, Belgium

**Keywords** Nitrogen transformation ·  
Tidal freshwater marsh ·  $^{15}\text{N}$  · Nitrification ·  
Denitrification

## Introduction

Tidal freshwater and oligohaline marshes are distinct features of inner estuaries and important nutrient filters. Nevertheless, the dynamics of nitrogen cycling in tidal freshwater marshes are not well understood (Bowden 1986; Merrill and Cornwell 2000). Most of what is known comes from tidal input/output studies, which are prone

to large errors and yield limited information about the nature and spatial and temporal distribution of the underlying processes.

The relatively new technique of tracing stable isotopes through intact aquatic ecosystems has provided increased understanding of N processing in a diverse range of systems such as groundwater plumes (Tobias et al. 2001), lakes (Kling 1994), streams (e.g. Peterson et al. 1997; Tank et al. 2000; Hamilton et al. 2001, Merriam et al. 2002; Ashkenas et al. 2004; Mulholland et al. 2004), and small estuaries (Holmes et al. 2000; Hughes et al. 2000; Tobias et al. 2003). Recently Gribsholt et al. (2005) applied the whole ecosystem  $^{15}\text{N}$  technique to a nutrient-rich tidal freshwater marsh system and revealed that nitrification is one of the fundamental processes regulating N-cycling during spring/early summer (May). While a substantial fraction of the flood water derived ammonium was biogeochemically transformed, relatively little nitrogen was retained within the marsh ecosystem. Although this  $^{15}\text{N}$  labeling experiment revealed whole ecosystem transformation rates that would have been difficult to obtain by traditional approaches (Schindler 1998; Holmes et al. 2000), it provided only a 'snapshot' of the ecosystem functioning. Seasonally variable factors, such as nutrient loading, developmental stage of macrophytes and associated microbial community, and temperature potentially influence the ecosystems nutrient transformation rates and pathways. Furthermore, due to the nature and scale of whole ecosystem labeling studies, true replication of these experiments is not possible, leaving the approach open to criticism, but they do provide ecological insight (Carpenter 1989; Schindler 1998). In order to (1) investigate seasonal differences in marsh nitrogen retention and transformation, and (2) examine the robustness of the whole ecosystem labeling approach, we conducted a second in situ  $^{15}\text{N}$ - $\text{NH}_4^+$  whole ecosystem labeling experiment in the same tidal freshwater marsh. This second experiment was deliberately scheduled in late summer (September), when macrophytes are in a flowering or early senescent state, to maximize the contrast with the first experiment in May, when plants were young and building up biomass.

Here we present the result of the water-phase component of this second marsh labeling experiment

and compare them to the May experiment. Our results revealed that while the marsh surface area was crucial for nitrification in May (Gribsholt et al. 2005), this was less pronounced in September. Denitrification, however, appeared more important in September compared to May. The similarity in the temporal and spatial patterns of  $^{15}\text{N}$  transformation to those observed in May implies that this type of unconfined, whole ecosystem stable isotope labeling studies are reproducible and thus providing robust biogeochemical information at the appropriate field scale.

## Methods

### Study area and $^{15}\text{N}$ addition

The study was conducted in the Tielrode tidal freshwater marsh fringing the Scheldt and Durme Rivers, Belgium ( $51^{\circ}06''$  N,  $4^{\circ}10''$  E). The Scheldt estuary and its feeding rivers are rich in nutrients (Soetaert et al. 2006) and fringing marshes in the Scheldt estuary are therefore characterized by large, fast-growing helophytes (Verhoeven et al. 2006). A  $3477\text{ m}^2$  triangular-shaped study marsh was enclosed by dikes on two sides and a 1 m high wooden wall on the remaining side. Flood water labeling and water sampling was conducted from a 4.5 m sampling platform spanning the width of the only creek entering the study area. A detailed description of the study area and the  $^{15}\text{N}$  addition procedure is found in Gribsholt et al. (2005).

Labeling was initiated when the first flood water arrived at the labeling platform on September 11, 2003. The label solution consisted of 1240 g of 10.7%  $^{15}\text{N}$  labeled ammonium sulfate ( $(\text{NH}_4)_2\text{SO}_4$ ) and 49 kg of the conservative tracer NaBr dissolved in 250 l of MilliQ  $\text{H}_2\text{O}$ . In total 180 l of label solution was added, corresponding to 1.41 mol  $^{15}\text{NH}_4^+$  and 333 mol  $\text{Br}^-$ . This increased the  $^{15}\text{N}$  content of the ammonium pool to 4.5% and increased the average total  $\text{NH}_4^+$  concentration from 20 to 34  $\mu\text{mol l}^{-1}$  (73%).

### Sampling, analysis and calculations

All creek water sampling and analysis was carried out according to the protocols described in Gribsholt et al. (2005). Briefly, samples

were collected 12 times during the main tide (flood + ebb) and 3 times during low tide (seepage phase) for analysis of  $\text{NH}_4^+$ ,  $\text{NO}_3^- + \text{NO}_2^-$ ,  $\text{N}_2\text{O}$ ,  $\text{N}_2$  and suspended particulate N (SPN) concentrations and N-isotopic composition, and for analysis of  $\text{Br}^-$  concentrations. Dissolved nitrous oxide ( $\text{N}_2\text{O}$ ) and dinitrogen ( $\text{N}_2$ ) concentrations and isotopic composition were determined in headspace gas by gas chromatography coupled to isotope ratio mass spectrometry (GC-IRMS) and elemental isotope ratio mass spectrometry (EA-IRMS), respectively. The isotopic composition of ammonium and nitrate were determined in 30 ml filtered samples in a two step ammonium diffusion procedure (Gribsholt et al. 2005) followed by EA-IRMS. Hereafter nitrate plus nitrite ( $\text{NO}_3^- + \text{NO}_2^-$ ) is referred to as nitrate ( $\text{NO}_3^-$ ). Bromide concentrations were determined by high-pressure ion chromatography. Dissolved oxygen, specific conductivity, temperature, pH and turbidity were recorded continuously (5 min intervals) during all tides using a Hydrolab Datasonde 3.

All measurements were conducted during five tides, namely prior to label addition ( $T_{-2}$ ) to establish natural abundance levels of  $^{15}\text{N}$ , at the time of label addition ( $T_0$ ) and at three subsequent tides ( $T_1$ ,  $T_2$  and  $T_5$ ). The subscript denotes the tide number relative to  $^{15}\text{N}$  addition. Water trapped (10 cm height intervals, Gribsholt et al. 2005) above 12 marsh sampling stations were analyzed for  $\text{Br}^-$  as described above.

Water phase nitrification rates (WNR) ( $T_{-1}$ , 6 times over the tidal cycle) were determined ex situ from transfer of  $^{15}\text{N}$  in ammonium to nitrate in dark bottle incubations (in situ temperature) spiked with  $^{15}\text{NH}_4\text{Cl}$  (98 atom%) to approximately 2% of the ambient  $\text{NH}_4^+$  concentration. Sediment denitrification was determined in four representative intact sediment cores (id. 15 cm) collected prior to  $T_0$  using the isotope pairing method (IPM) of Nielsen (1992). Cores were flooded with creek water entering the site at the onset of  $T_0$ -flood ( $[\text{NH}_4^+] = 7 \mu\text{mol l}^{-1}$ ;  $[\text{NO}_3^-] = 335 \mu\text{mol l}^{-1}$ ) spiked with  $^{15}\text{NO}_3^-$  (500–800  $\mu\text{l}$   $1.17 \text{ mol}^{-1}$ , 99%  $\text{Na}^{15}\text{NO}_3^-$ , doubling the ambient  $[\text{NO}_3^-]$ ) and incubated (closed, dark, stirred) for ~6 h. Total denitrification was calculated from linear concentrations changes of excess  $^{29}\text{N}_2$  and  $^{30}\text{N}_2$  over time.

Water, total nitrogen and  $^{15}\text{N}$  budgets for each tide were calculated from the measured water flows, water heights and total nitrogen and  $^{15}\text{N}$  pool sizes (Table 1). The total volume of water covering the study area in a given tide, the duration of submergence and surface area with water cover were calculated from the digital terrain model (Gribsholt et al. 2005).

Net ecosystem nitrification rate (ENR) was calculated from the linear increase in isotopic enrichment of  $\text{NO}_3^-$  during  $T_0$  ebb ( $\text{ENR}_{\text{regression}}$ ), and from the net transfer of  $^{15}\text{N}$  from the added ammonium pool to the nitrate pool over the first tide ( $T_0$ ) ( $\text{ENR}_{\text{mass-balance}}$ ) according to Equations 1 and 2 in Gribsholt et al. (2005), respectively. System based  $\text{N}_2\text{O}$  production rate was estimated using a similar approach. Air–water exchange fluxes of  $^{15}\text{N}_2\text{O}$  and  $^{15}\text{N}_2$  were calculated from the product of gas transfer or piston velocity ( $k$ ), and the available gas exchange water surface area determined from water height and digital terrain model (Gribsholt et al. 2005).

## Results

### Hydrodynamics and creek characterization

The study area is only flooded by the highest tides, and because most tides were lower than predicted, a small part of the study area remained air-exposed (Table 1). As expected, flooding duration and water volume increased with maximum tidal height, and ebb lasted 33–45% longer than flood. While the water budgets were almost closed for all tides except the very low  $T_5$ -tide, the calculated flood and ebb volumes were significantly lower than those estimated by the GIS model. The discrepancy increased with decreasing tidal heights. Correcting for a 15% water balance underestimation suggested by the  $T_0$  bromide mass balance (see below) reduces these discrepancies by 40–80% (Table 1). A portion of the remaining difference ( $189 \pm 22 \text{ m}^3$ ) may represent transient storage in sediment crevices and between vegetation. Some can also be attributed to an overestimation by the digital terrain model, which does not take into account the volume of the vegetation and plant litter. Furthermore, even

**Table 1** Duration of main tide (flood and ebb), maximum tidal water velocity (creek center), relative area inundated, maximum water height above creek bed (2.47 m above mean sea level) below measuring platform, water volume estimated from the digital terrain model and calculated water budget computed by mass balance model during the tides

Tide (nr.)	Duration (min)		Maximum velocity (cm s <sup>-1</sup> )		Area inundated (%)	Water height (cm)	Water volume <sup>a</sup> (m <sup>3</sup> )	Water budget			Import in % of total volume <sup>b</sup> (%)	Export in % of total volume <sup>c</sup> (%)	
	Flood	Ebb	Flood	Ebb				Flood (m <sup>3</sup> )	Ebb (m <sup>3</sup> )	Seepage (m <sup>3</sup> )			Balance (m <sup>3</sup> )
T <sub>-2</sub>	80	104	23	32	98	103	1277	904	880	44	-20 (-2.2)	71 [83]	72 [85]
T <sub>0</sub>	79	107	18	37	98	103	1277	911	895	46	-30 (-3.3)	71 [84]	74 [87]
T <sub>1</sub>	73	103	16	25	95	95	986	667	641	42	-16 (-2.4)	68 [80]	69 [81]
T <sub>2</sub>	86	120	24	35	100	122	1987	1562	1479	52	31 (2.0)	79 [92]	77 [91]
T <sub>5</sub>	59	78	22	18	78	81	532	307	215	47	45 (14.7)	58 [68]	49 [58]

Values in parenthesis are balances in percentage of flood. Values in [] are corrected for 15% mass balance underestimation (see text)

<sup>a</sup>Calculated from the digital terrain model and max water height

<sup>b</sup>Calculated floodwater volume from mass balance model in percentage of water volume estimated from <sup>a</sup>

<sup>c</sup>Calculated ebb water volume + seepage from mass balance model in percentage of water volume estimated from <sup>a</sup>

slight elevation errors can lead to errors in estimating tidal prism.

The temporal patterns of N (dissolved and particulate) concentrations were generally similar among all tides, and resembled those observed in May (Gribsholt et al. 2005). Only the ammonium and directly correlated ( $R^2 = 0.76$ ,  $P < 0.001$ ) N<sub>2</sub>O concentrations (data not shown) varied significantly between tides. Following an initial decrease, ammonium concentration (Fig. 1a) showed a bell-shaped distribution pattern over the tidal cycle, with maximum concentrations (32–52  $\mu\text{mol l}^{-1}$ ) around the turn of the tide. An exception is the very low T<sub>5</sub>-tide, which showed a more erratic temporal pattern. The exceptional peak observed in T<sub>0</sub>-[NH<sub>4</sub><sup>+</sup>] (68  $\mu\text{mol l}^{-1}$ ) was due to excessive label addition at the turn of the tide (see below). The nitrate concentrations generally showed a bimodal distribution curve with maxima (300–330  $\mu\text{mol l}^{-1}$ ) mid-flood and -ebb (Fig. 1b). Ebb nitrate concentrations gradually decreased to ~200  $\mu\text{mol l}^{-1}$  and continued to decrease during seepage, when [NH<sub>4</sub><sup>+</sup>] concentrations increased from < 10 to ~20  $\mu\text{mol l}^{-1}$ . Overall the dissolved inorganic nitrate pool (DIN = NH<sub>4</sub><sup>+</sup> + NO<sub>3</sub><sup>-</sup> +

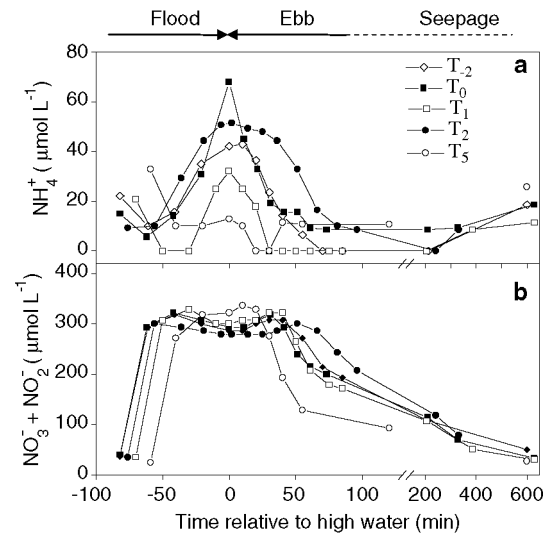


**Fig. 1** Concentrations of (a) dissolved ammonium (NH<sub>4</sub><sup>+</sup>) and (b) dissolved nitrate and nitrite (NO<sub>3</sub><sup>-</sup> + NO<sub>2</sub><sup>-</sup>) in the creek below the sampling platform as a function of time relative to maximum tidal height in all five tides. The three phases of the tidal cycle (flood, ebb and seepage) are indicated above the figure, with arrow indicating the direction of the water flow

$\text{NO}_2^-$ ) was relatively constant ( $330\text{--}340 \mu\text{mol l}^{-1}$ ) for the main duration of all tides, with  $\text{NH}_4^+$  accounting for 3–11% of DIN.

While the suspended nitrogen concentrations (SPN) generally decreased (from  $50\text{--}90$  to  $0\text{--}20 \mu\text{mol l}^{-1}$ ) over the tidal cycle, the turbidity remained relatively constant ( $\sim 200$  NTU, nephelometric turbidity units), and the water was always highly  $\text{O}_2$  under-saturated (7.5–52% saturation,  $22\text{--}159 \mu\text{mol l}^{-1}$ ), with concentrations inversely correlated to water height ( $R^2 = 0.94$ ,  $P < 0.001$ ) (data not shown). Water temperature, pH, and conductivity varied from  $16\text{--}19^\circ\text{C}$ , 7.3–7.6, and  $1.2\text{--}2.1 \text{ mS m}^{-1}$  between tides, respectively.

### Label distribution

Uniform bromide concentrations in the bulk part of  $T_0$  ebb ( $0.35 \pm 0.05 \text{ mmol l}^{-1}$ ) and in water traps ( $0.38 \pm 0.09 \text{ mmol l}^{-1}$ ,  $n = 28$ ) confirm a successful even distribution of label. An initial peak ( $0.77 \text{ mmol l}^{-1}$ ) in  $T_0$  ebb bromide concentration (directly after the  $\sim 80$  min period of label addition to the flood water) revealed label addition in excess around the abrupt turn of the tide. This, however, is of little consequence since this last labeled body of flood water, quickly leaves the creek, before mixing with the main body of water covering the study area. Recovery of the added  $\text{Br}^-$  in the  $T_0$  mass balance was 85%, suggesting that the  $T_0$  ebb water volume was underestimated. Elevated initial flood water [ $\text{Br}^-$ ] ( $27\text{--}74 \mu\text{mol l}^{-1}$ ) in subsequent tides compared to natural abundance levels ( $12 \pm 4 \mu\text{mol l}^{-1}$ ), together with an increase (up to  $50 \mu\text{mol l}^{-1}$ ) during late ebb and seepage, resulted in a completely closed (i.e. no net import or export) bromide budget for these tides ( $T_1\text{--}T_5$ ).

The ammonium pool in the  $T_0$  ebb water was highly enriched in  $^{15}\text{N}$  ( $\sim 5000\text{--}11000\text{‰}$ ). Except for the initial peak in excess concentration of  $^{15}\text{NH}_4^+$  ( $1.6 \mu\text{mol l}^{-1}$ ), which is attributed to over-labeling around the turn of the tide (see above), the excess  $^{15}\text{NH}_4^+$  concentration was relatively constant ( $0.6 \mu\text{mol l}^{-1}$ ) for the main duration of  $T_0$  -ebb (Fig. 2a). Removal of  $^{15}\text{N}$  from the ammonium pool during  $T_0$  was, however, clearly evident from the decrease in  $^{15}\text{NH}_4^+$ :  $\text{Br}^-$  concentration

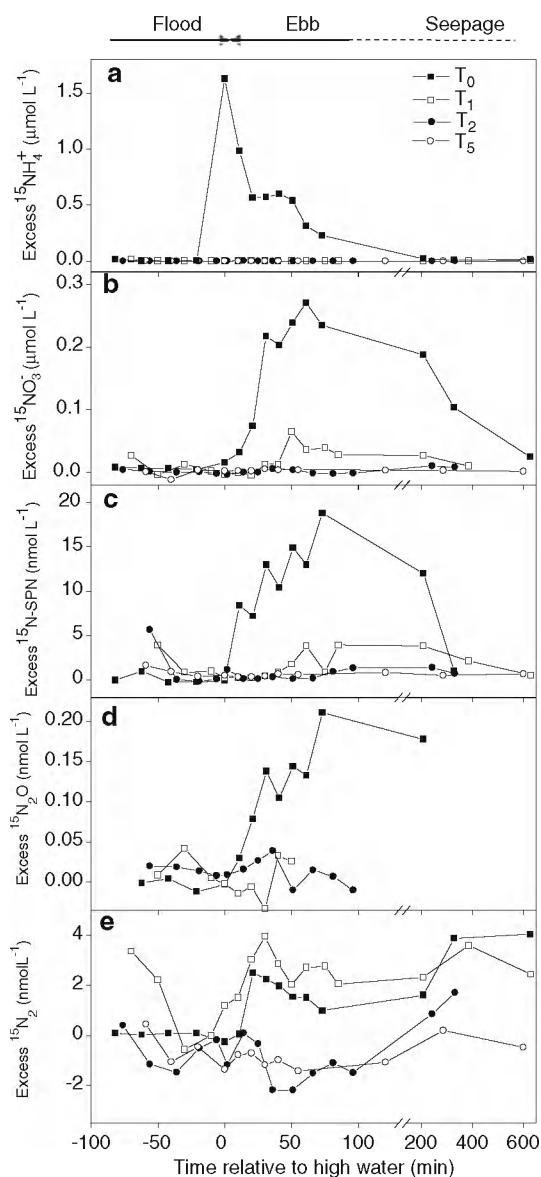


**Fig. 2** Excess  $^{15}\text{N}$  concentration of (a)  $^{15}\text{NH}_4^+$ , (b)  $^{15}\text{NO}_3^-$ , (c)  $^{15}\text{N}$ -SPN, (d)  $\text{N}_2\text{O}$ , and (e)  $\text{N}_2$  in the flood water. The three phases of the tidal cycle (flood, ebb and seepage) are indicated above the figure, with arrow indicating the direction of the water flow

ratio from  $3.0 \times 10^{-3}$  initially to  $0.7 \times 10^{-3}$  at the end of the ebb tide (Fig. 3a). In the seepage water the excess  $^{15}\text{N}\text{-NH}_4^+$  concentration decreased by two orders of magnitude (to  $10 \text{ nmol l}^{-1}$ ). In subsequent tides the initial flood sample of  $T_1$  showed significant enrichment (172 ‰) of the ammonium pool, and  $T_1$  ebb and seepage water was also significantly enriched (up to 57 ‰).

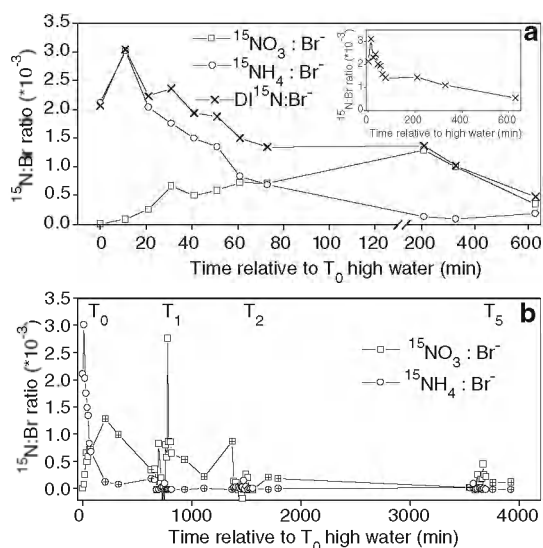


**Fig. 3** (a) Ratio between excess  $^{15}\text{N}$  in  $\text{NH}_4^+$ ,  $\text{NO}_3^-$  and DIN and conservative tracer  $\text{Br}^-$  concentrations during  $T_0$ -ebb and -seepage (insert shows  $\text{DI}^{15}\text{N} : \text{Br}^-$  on an unbroken timescale), and (b) ratio between excess  $^{15}\text{N}$  in  $\text{NH}_4^+$  and  $\text{NO}_3^-$  and the conservative tracer  $\text{Br}^-$  concentrations from end of label addition ( $T_0$ -max) to  $T_5$ . Symbols with (+) indicate seepage phase. Note the different scales on the x-axis

Slight enrichment was even detectable in the  $T_2$  ebb and seepage water (up to 28 ‰).

Isotopic enrichment of the nitrate pool was observed immediately around the turn of the  $T_0$ -tide. During  $T_0$  ebb the excess  $^{15}\text{NO}_3^-$  concentrations increased linearly ( $R^2 = 0.82$ ,  $P < 0.01$ ) to  $\sim 0.27 \mu\text{mol l}^{-1}$  (Fig. 2b), but subsequently decreasing one order of magnitude during

seepage. The isotopic enrichment and excess  $^{15}\text{N}$  concentration of the dissolved nitrous oxide ( $\text{N}_2\text{O}$ ) pool were linearly correlated ( $R^2 = 0.73$ ,  $P < 0.01$  and  $R^2 = 0.94$ ,  $P < 0.001$ , respectively) with those of nitrate (Fig. 2d). Enrichment of the nitrate pool during  $T_0$  is further evident from the linear ( $R^2 = 0.82$ ,  $P < 0.001$ ) increase in the  $^{15}\text{NO}_3^- : \text{Br}^-$  concentration ratio (Fig. 3a), and a similar linear increase ( $R^2 = 0.95$ ,  $P < 0.001$ ) was observed in the  $^{15}\text{N}_2\text{O} : \text{Br}^-$  concentration ratio (data not shown). Nitrate in  $T_1$  initial flood water as well as seepage was significantly enriched, as also evident from the high  $\text{NO}_3^- : \text{Br}^-$  concentration ratio (Fig. 3b). The isotopic enrichment and pattern of excess  $^{15}\text{N}$  in the particulate nitrogen pool (SPN) mimicked that of nitrate, but excess- $^{15}\text{N}$ -SPN was one order of magnitude lower. A slight increase (1–2 ‰) in  $^{15}\text{N}$  of the  $\text{N}_2$ -pool was observed during  $T_0$  and  $T_1$ , with an erratic temporal pattern in excess  $^{15}\text{N}_2$  concentrations (Fig. 2e).

#### Nitrogen transformation rates and the fate of N

The  $^{15}\text{N}$  mass balance budget revealed that half of the added  $^{15}\text{NH}_4^+$  label was either transformed or taken up by marsh biota, while the other half (51%) was exported as ammonium (unprocessed) during the first tide (Table 2). Nitrification was quantitatively the most important transformation process for  $^{15}\text{N}$ . After  $T_0$ , 7.7% of the added  $^{15}\text{N}$  was recovered in the nitrate pool, corresponding

**Table 2**  $^{15}\text{N}$  mass balance budget

Compartment	$T_0$ (mmol)		$T_1$ (mmol)		$T_2$ (mmol)		$T_5$ (mmol)	
Label input	1409	(100)						
$^{15}\text{N}$ exported unchanged (as $^{15}\text{NH}_4$ )	715	(51)	715	(51)	715	(51)	716	(51)
$^{15}\text{N}$ transformed	694	(49)	694	(49)	694	(49)	693	(49)
$^{15}\text{NO}_3^- + ^{15}\text{NO}_2^-$	109	(7.7)	113	(8.0)	115	(8.2)	117	(8.3)
$^{15}\text{N}_2\text{O}$ —dissolved	0.1	(0.0)	0.1	(0.0)	0.1	(0.0)	0.1	(0.0)
$^{15}\text{N}_2\text{O}$ —water-air	0.1	(0.0)	0.1	(0.0)	0.1	(0.0)	0.1	(0.0)
$^{15}\text{N}_2$ —dissolved	1.7	(0.1)	3.2	(0.2)	2.4	(0.2)	2.4	(0.2)
$^{15}\text{N}_2$ —water-air	6.2	(0.4)	13.4	(1.0)	13.4	(1.0)	13.4	(1.0)
SP $^{15}\text{N}$	9.5	(0.7)	9.1	(0.6)	8.2	(0.6)	9.2	(0.7)
SINKS—stored	56	(3.9)	138	(9.8)	53	(3.8)	57	(4.1)
Balance not accounted for	512	(36)	418	(30)	502	(36)	494	(35)

Recovery in the various N-pools after  $T_0$ ,  $T_1$ ,  $T_2$  and  $T_5$  in September 2003 are cumulative, except for SINK where actual stocks are listed. Numbers in parenthesis are percentage of the total  $^{15}\text{N}$  added

to an in situ whole ecosystem nitrification rate ( $\text{ENR}_{\text{mass-balance}}$ ) of  $0.9 \mu\text{mol l}^{-1} \text{h}^{-1}$  (Table 3). Based on the linear increase ( $R^2 = 0.93$ ,  $P < 0.001$ ) in excess  $^{15}\text{NO}_3^-$  concentration during  $T_0$ -ebb (Fig. 2b), a higher ( $2.5 \mu\text{mol l}^{-1} \text{h}^{-1}$ ) ENR was obtained ( $\text{ENR}_{\text{regression}}$ , Table 3). Both estimates are higher than the average rate ( $0.5 \pm 0.3 \mu\text{mol l}^{-1} \text{h}^{-1}$ ) measured in the water phase (WNR).

Although the dissolved nitrous oxide pool was significantly labeled, it accounted for  $<0.01\%$  due to its low concentrations, and water–air exchange could only account for another  $\sim 0.01\%$   $^{15}\text{N-N}_2\text{O}$  loss to the atmosphere. The whole ecosystem nitrous oxide production rate was  $0.6\text{--}1.7 \text{mmol l}^{-1} \text{h}^{-1}$ , resulting in a system based  $\text{NO}_3^- : \text{N}_2\text{O}$  ratio of 1407:1– 1462:1. A slightly larger fraction ( $\sim 0.22\%$  of label) was recovered in the dissolved  $\text{N}_2$ -pool, with  $T_1$  being most enriched. Estimated water–air exchange could account for up to  $6.2 \text{mmol } ^{15}\text{N-N}_2$  to the atmosphere, corresponding to  $0.44\%$  of added label during  $T_0$  and a further  $7.1 \text{mmol}$  during  $T_1$ . Cumulative  $^{15}\text{N}_2$  loss (assuming a piston velocity ( $k$ ) of  $50 \text{cm h}^{-1}$ ) could account for as much as  $1\%$  of the added label. The closed core incubations revealed high sediment denitrification rates ( $0.4\text{--}2.0 \text{mmol N}_2 \text{m}^{-2} \text{h}^{-1}$ ), with highest rates observed in unvegetated sediments. Assuming an average denitrification rate of  $1.0 \text{mmol m}^{-2} \text{h}^{-1}$  throughout the entire  $3477 \text{m}^2$  experimental marsh, and that  $0.1\%$  of the nitrate pool was labeled (based on measured  $[\text{excess } ^{15}\text{NO}_3^-]/[\text{NO}_3^-]$ ), approximately  $3\%$  ( $42 \text{mmol}$ ) of the

added  $^{15}\text{N}$  label could be removed through denitrification during the first tide.

About  $1\%$  of the label was recovered in the suspended particulate pool (SPN) and collectively the marsh sinks (sediments, plants, roots, plant litter) accounted for  $4\text{--}10\%$  of the added label (Gribsholt et al. unpublished data). A large fraction ( $30\text{--}36\%$ ) of the label could not be recovered and is most likely transferred to the dissolved organic nitrogen (DON) pool (and subsequently exported during ebb) or denitrified during emersion (and then lost to the atmosphere) (see Gribsholt et al. 2005). Correcting the  $^{15}\text{N}$  mass balance budgets for the  $15\%$  underestimation suggested by the  $T_0$  ebb bromide budget (see above), reduces the fraction that is unaccounted for to  $20\text{--}26\%$  and increases  $\text{ENR}_{\text{mass balance}}$  to  $1.01 \mu\text{mol l}^{-1} \text{h}^{-1}$ .

## Discussion

The data presented here are from an experiment conducted in September 2003, and despite differences in  $\text{NO}_3^- : \text{NH}_4^+$  ratios and macrophyte community composition, the temporal and spatial patterns of  $^{15}\text{N}$  transformation in the water phase component of the system are remarkably similar to those observed in May 2002 (Gribsholt et al. 2005). Among the most striking similarities are the tidal patterns of concentrations; the patterns of label distribution; the instant and linear increase in isotopic enrichment of  $\text{NO}_3^-$  and  $\text{N}_2\text{O}$ ; the instant, linear increase in the  $^{15}\text{NO}_3^- : \text{Br}^-$

**Table 3** Nitrification rate in the water phase (WNR,  $n = 6$ ) and whole marsh ecosystem (ENR) in May and September

Compartment	Method	Nitrification rate ( $\mu\text{mol l}^{-1} \text{h}^{-1}$ )	
		May <sup>a</sup>	September
Water phase	$^{15}\text{N}$ bottle incubations	$0.5 \pm 0.1$	$0.5 \pm 0.3$
Whole ecosystem	$\text{ENR}_{\text{regression}}^{\text{b}}$	4.6 (2.4)	2.5 (0.7)
	$\text{ENR}_{\text{mass-balance}}^{\text{c}}$	2.0 (1.1)	0.9 (0.2)
	Nutrient mass balance	$-7.3$ to $21.2$	$-3.3$ to $22.0$

Numbers in parenthesis are rates recalculated to rate per inundated marsh surface area ( $\text{mmol m}^{-2} \text{h}^{-1}$ ). Water phase incubations were done during  $T_{-2}$ , while whole ecosystem rates were determined from  $T_0$

<sup>a</sup>Data from Gribsholt et al. 2005

<sup>b</sup>Determined according to Equation #1 in Gribsholt et al. 2005, see text for details

<sup>c</sup> Determined according to Equation #2 in Gribsholt et al. 2005, see text for details

<sup>d</sup>All tides, derived from  $\text{NO}_3^-$  mass balance

ratio; and a very high  $\text{NO}_3^-$ :  $\text{N}_2\text{O}$  ratio. The striking similarity in label distribution and high recovery rates on both occasions support that our results are quite robust and the September experiment presented here thus validates previous findings (Gribsholt et al. 2005).

However, there are also conspicuous differences, including the much lower ammonium concentrations; shorter inundation durations; a significantly higher degree of labeling; and a significantly higher recovery of  $^{15}\text{N}$  in the dinitrogen pool in September compared to May. The discussion focuses on these main similarities and differences.

Ideally, flooding regimes and degree of labeling should have been similar on both occasions. Unfortunately, the September tides were lower than predicted. Consequently marsh inundation periods were shorter compared to May, and a significantly smaller reactive plant and litter surface area was inundated. Thus nitrification and denitrification in the periphyton on plant shoots and litter, where rates (expressed per shoot area) are very high (Erikson and Weisner 1999; Toet et al. 2003), may therefore have been limited in September compared to May. Thus rates of ecosystem nitrification and denitrification would potentially have been higher in September if the inundation regime was similar to the May campaign. The difference in total amounts of ammonium processed would thus have been smaller (Fig. 4b, see below). This effect may, however, be counteracted by a reduced importance of periphyton associated nitrogen processing in September due to increased shading (Toet et al. 2003).

The value of using in situ tracer additions to study ecosystem nutrient dynamics is that the processes can be examined under ambient conditions, without making a priori or biased assumptions about the most important ecosystems compartments and the artifacts resulting from stimulation of process rates by temporarily increasing nutrient concentrations (nutrient enrichment studies), or artifacts associated with the use of enclosures (microcosm studies) (Mulholland et al. 2000). In the September  $^{15}\text{N}$  labeling experiment, however, the lower than expected tidal inundation combined with low

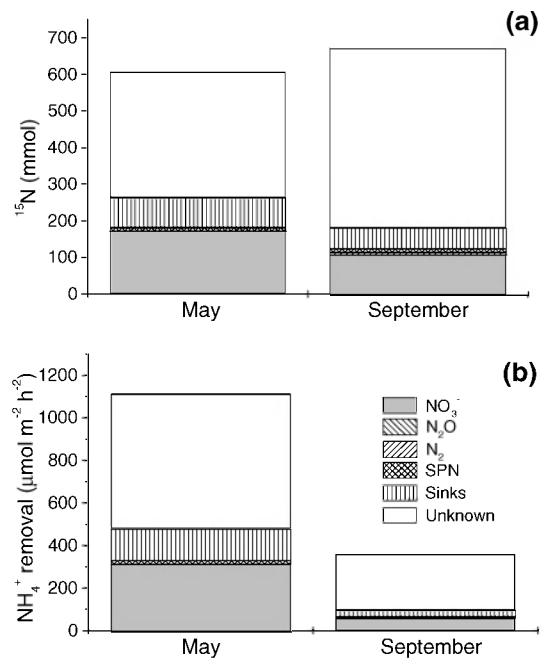


**Fig. 4** (a) Amount of recovered  $^{15}\text{N}$  in the various pools after  $T_0$  in May and September (not exported as  $^{15}\text{NH}_4^+$ ), and (b) average total marsh ammonium transformation rates based on recovery of  $^{15}\text{N}$  label after one tide ( $T_0$ )

ambient ammonium concentrations resulted in a substantial (73%) increase in the total average ammonium concentration and a higher degree of  $^{15}\text{N}$  labeling (4.5%) compared to that in our previous study (1.5%). Thus the basic assumption that the added  $^{15}\text{N}$  label does not accelerate in situ rates but merely substitutes for ambient  $^{14}\text{N}$  may not be entirely met in the September experiment and ammonium process rates may have been slightly overestimated. However, in this very nutrient-rich system ammonium is likely not limiting, and despite the induced minor perturbation the isotope labeling approach clearly revealed in situ pathways not otherwise obtainable. Moreover, the in situ  $^{15}\text{N}$  addition approach is perhaps the only way to obtain reliable whole system N-transformation rates, because conventional mass balance approaches are usually prone to such error that few conclusions can be drawn.

The relative fate of the added  $^{15}\text{N}$  was surprisingly similar in May and September (Fig. 4a). On both occasions nitrate was the most important pool for processed  $^{15}\text{NH}_4^+$ , accounting for 8.7 and 7.7% of the added label, or 32 and 17% of the

transformed label (i.e. not exported as  $^{15}\text{NH}_4^+$ ) in May and September, respectively. Nitrification is directly evident from the direct transfer of  $^{15}\text{N}$  from the added ammonium pool to the nitrate pool (Fig. 2b). As in May, enriched nitrate was also exported from the marsh in the following tides, and while the dissolved ammonium was only labeled during  $T_0$  in May, some enrichment was also observed in subsequent ebb tides during September. This suggests that the marsh acts as at least a temporary sink for N, either through pore water DIN exchange, sorption or rapid assimilation by microbes and subsequent mineralization. Whole ecosystem nitrification was lower in September than in May (Table 3), while water-column nitrification was similar, indicating that sediment nitrification was lower. Bodelier et al. (1996) reported that oxygen releasing plants (like those found in the marsh) stimulate the numbers and activity of nitrifying bacteria in sediments during spring and early summer, but not in late summer where a combination of an increasing oxygen and/or nitrogen demand by bacteria in the sediment in concert with a decrease in the amount of oxygen released by plants results in inhibition of nitrifiers over the course of the growing season. Less contact between flood water and periphyton, due to less extensive submergence, could also contribute to the observed differences as discussed above. Furthermore, benthic algae cover was considerably reduced in September compared to May. Photoautotrophic benthic oxygen production could potentially enhance benthic nitrification in May, whereas more reduced conditions in surface sediment in September would favor denitrification (see below).

Concurrent with the isotopic enrichment of the nitrate pool a clear increase in  $\delta^{15}\text{N}_2\text{O}$  occurred. Similar to the May study the increase in  $\delta^{15}\text{N}_2\text{O}$  even exceeded the increase in  $\delta^{15}\text{NO}_3^-$ , indicating that nitrous oxide production is largely due to a direct transfer from ammonium via nitrification (promoted by hypoxic conditions; Goreau et al. 1980; de Bie et al. 2002), rather than denitrification. The slightly higher average system based  $\text{NO}_3^-:\text{N}_2\text{O}$  ratios compared to May (1435:1 vs. 1052:1), might suggest that relatively more of the  $\text{N}_2\text{O}$  produced via nitrification is consumed by denitrification in September. However,  $\text{NO}_3^-:$

$\text{N}_2\text{O}$  ratio also depends on other environmental conditions, in particular low oxygen availability (de Bie et al. 2002).

Contrary to May, a significant, albeit low, isotopic enrichment in dissolved  $\text{N}_2$  was observed not only during  $T_0$  but also in subsequent tides, suggesting that denitrification was more important in September. Sediment core incubation supports this, as rates in unvegetated creek bank sediment were 4 times higher in September ( $2.0 \text{ mmol m}^{-2} \text{ h}^{-1}$ , isotope pairing method) than in May ( $0.5 \text{ mmol m}^{-2} \text{ h}^{-1}$ , membrane inlet mass spectrometry), but we cannot exclude that this difference is partly related to difference in methodology. However, ecosystem based results may be biased because the much higher degree of labeling allowed for a better detection of dissolved  $^{15}\text{N}_2$  in September, and only a limited number of sediment core denitrification measurements were conducted. Direct estimates of ecosystem denitrification cannot be obtained from our  $^{15}\text{N}$  data, since the marsh was labeled with  $^{15}\text{NH}_4^+$  rather than  $^{15}\text{NO}_3^-$ , and since sediment–air gas exchange during emersion was not determined. However, the conservative estimate (based on average denitrification rate in core incubations and assuming 0.1%  $^{15}\text{N}$  labeling of the nitrate pool; see Results) of  $42 \text{ mmol } ^{15}\text{N}_2$  ( $\sim 3\%$  of the added label) potentially being produced in the first tide is in good agreement with the water–air flux calculations and thus supports their validity. Furthermore, an enhanced importance of denitrification in September is supported by the higher  $\text{NO}_3^-:\text{N}_2\text{O}$  ratios as discussed above.

Although the total amount of  $^{15}\text{N}$ , and the relative distribution of  $^{15}\text{N}$  recovered in the various compartments was quite similar between the two campaigns (Fig. 4a), the corresponding total ammonium processing rates on a marsh surface area basis varied greatly (Fig. 4b). This is mainly due to a combination of a 5 times lower total in situ flood water ammonium pool and a higher relative  $^{15}\text{N}$  (4.5% of the ammonium pool) concentration in September. Thus, the absolute amount of ammonium processed in the marsh was 3 times higher, and  $>5$  times more ammonium was nitrified, in May compared to September. These findings suggest that flood water ammonium concentration is the key determinant for

ammonium removal in tidal freshwater marsh ecosystems (given similar temperature and water retention time).

**Acknowledgements** This study received funding from the Flemish–Dutch co-operation on Coastal Research (VLANEZO) under the Flemish and Dutch Science Foundations FWO-NWO. We thank the staff at the NIOO-CEME analytical laboratory for their assistance. This is publication number 3820 from the NIOO-CEME.

## References

- Ashkenas LR, Johnson SL, Gregory SV, Tank JL, Wollheim WM (2004) A stable isotope tracer study of nitrogen uptake and transformation in a old-growth forest stream. *Ecology* 86:1725–1739
- de Bie MJM, Middelburg JJ, Starink M, Laanbroek HJ (2002) Factors controlling nitrous oxide at the microbial community and estuarine scale. *Mar Ecol Prog Ser* 240:1–9
- Bodelier PLE, Libochant JA, Blom CWPM, Laanbroek HJ (1996) Dynamics of nitrification and denitrification in root-oxygenated sediments and adaptation of ammonia-oxidizing bacteria to low-oxygen or anoxic habitats. *Appl Environ Microbiol* 62:4100–4107
- Bowden WB (1986) Nitrification, nitrate reduction, and nitrogen immobilization in a tidal freshwater marsh sediment. *Ecology* 67:88–99
- Carpenter SR (1989) Replication and treatment strength in whole lake experiments. *Ecology* 70:453–463
- Eriksson PG, Weisner SEB (1999) An experimental study on effects of submersed macrophytes on nitrification and denitrification in ammonium-rich aquatic systems. *Limnol Oceanogr* 44:1993–1999
- Goreau TJ, Kaplan WA, Wofsy SC, McElroy MB, Valois FW, Watson SW (1980) Production of  $\text{NO}_2^-$  and  $\text{N}_2\text{O}$  by nitrifying bacteria at reduced concentration of oxygen. *Appl Environ Microbiol* 40:526–532
- Gribsholt B, Boschker HTS, Struyf E, Andersson M, Trammer A, De Brabandere L, van Damme S, Brion N, Meire P, Dehairs F, Middelburg JJ, Heip C (2005) Nitrogen processing in a tidal freshwater marsh: a whole ecosystem  $^{15}\text{N}$  labeling study. *Limnol Oceanogr* 50:1945–1959
- Hamilton SK, Tank JL, Raikow DF, Wollheim WM, Peterson BJ, Webster JR (2001) Nitrogen uptake and transformation in a midwestern US stream: a stable isotope enrichment study. *Biogeochemistry* 54:297–340
- Holmes RM, Peterson BJ, Deegan LA, Hughes JE, Fry B (2000) Nitrogen biogeochemistry in the oligohaline zone of a New England estuary. *Ecology* 81:416–432
- Hughes JE, Deegan LA, Peterson BJ, Holmes RM, Fry B (2000) Nitrogen flow through the food web in the oligohaline zone of a New England estuary. *Ecology* 81:433–452
- Kling GW (1994) Ecosystem-scale experiments. The use of stable isotopes in fresh waters. In: Baker LA (ed) *Environmental chemistry of lakes and reservoirs*. American Chemical Society pp 91–120
- Merriam JL, McDowell WH, Tank JL, Wollheim WM, Crenshaw CL and Johnson SL (2002) Characterizing nitrogen dynamics, retention and transport in a tropical rainforest stream using an in situ  $^{15}\text{N}$  addition. *Freshwat Biol* 47:143–160
- Merrill JZ, Cornwell J (2000) The role of oligohaline marshes in estuarine nutrient cycling. In: Weinstein MP, Kreeger DA (eds) *Concepts and controversies in tidal marsh ecology*. Kluwer Academic Publishers, pp 425–441
- Mulholland PJ, Tank JL, Sanzone DM, Wollheim WM, Peterson BJ, Webster JR, Meyer JL (2000) Nitrogen cycling in a forest stream determined by a  $^{15}\text{N}$  tracer addition. *Ecol Monogr* 70:471–493
- Mulholland PJ, Valett HM, Webster JR, Thomas SA, Cooper LW, Hamilton SK, Peterson BJ (2004) Stream denitrification and total nitrate uptake rates measured using a field  $^{15}\text{N}$  tracer addition approach. *Limnol Oceanogr* 49:809–820
- Nielsen LP (1992) Denitrification in sediment determination from nitrogen isotope pairing. *FEMS Microb Ecol* 86:357–362
- Peterson BJ, Bahr M, Kling GW (1997) A tracer investigation of nitrogen cycling in a pristine tundra river. *Can J Fish Aquat Sci* 54:2361–2367
- Schindler DW (1998) Replication versus realism: the need for ecosystem-scale experiments. *Ecosystems* 1:323–334
- Soetaert K, Middelburg JJ, Heip C, Meire P, Van Damme S, Maris T (2006) Long-term change in dissolved inorganic nutrients in the heterotrophic Scheldt estuary (Belgium, the Netherlands). *Limnol Oceanogr* 51:409–423
- Tank JL, Meyer JL, Sanzone DM, Mulholland PJ, Webster JR, Peterson BJ, Wollheim WM and Leonard NE (2000) Analysis of nitrogen cycling in a forest stream during autumn using a  $^{15}\text{N}$ -tracer addition. *Limnol Oceanogr* 45:1013–1029
- Tobias CR, Macko SA, Anderson IC, Canuel EA, Harvey JW (2001) Tracking the fate of a high concentration groundwater nitrate plume through a fringing marsh: A combined groundwater tracer and an in situ isotope enrichment study. *Limnol Oceanogr* 46:1977–1989
- Tobias CR, Cieri M, Peterson BJ, Deegan LA, Vallino J, Hughes JE (2003) Processing watershed-derived nitrogen in a well-flushed New England estuary. *Limnol Oceanogr* 48:1766–1778
- Toet S, Huibers LHFA, Van Logtestijn RSP, Verhoeven JTA (2003) Denitrification in the periphyton associated with plant shoots in the sediment of a wetland system supplied with sewage treatment plant effluent. *Hydrobiologia* 501:29–44
- Verhoeven JTA, Arheimer B, Yin C, Hefting MM (2006) Regional and global concerns over wetlands and water quality. *Trends Ecol Evol* 21:96–103